

^{18}F -fluorodeoxyglucose and ^{18}F -sodium fluoride positron emission tomography imaging in assessing early stages of aortic valve degeneration after transcatheter aortic valve implantation

Danuta Sorysz^{1,2}, Artur Dziewierz^{1,2}, Marta Opalińska^{3,4}, Anna Sowa-Staszczak^{3,4}, Anna Grochowska⁵, Krzysztof P. Malinowski^{6,7}, Natalia Maruszak², Stanisław Bartuś^{1,2}, Dariusz Dudek^{1,7}

1 Clinical Department of Cardiology and Cardiovascular Interventions, University Hospital, Kraków, Poland

2 Second Department of Cardiology, Institute of Cardiology, Jagiellonian University Medical College, Kraków, Poland

3 Clinical Department of Endocrinology, Oncological Endocrinology and Nuclear Medicine, University Hospital, Kraków, Poland

4 Department of Endocrinology, Jagiellonian University Medical College, Kraków, Poland

5 Department of Radiology, University Hospital, Kraków, Poland

6 Department of Bioinformatics and Telemedicine, Jagiellonian University Medical College, Kraków, Poland

7 Center for Digital Medicine and Robotics, Jagiellonian University Medical College, Kraków, Poland

KEY WORDS

imaging, positron emission tomography, transcatheter aortic valve implantation, valve degeneration, valve durability

ABSTRACT

INTRODUCTION Transcatheter aortic valve implantation (TAVI) is a standard treatment for severe aortic stenosis, primarily in elderly patients. With an increasing number of procedures and younger patients, understanding the valve degeneration and its risk factors becomes crucial.

OBJECTIVES We aimed to utilize ^{18}F -sodium fluoride (^{18}F -NaF) and ^{18}F -fluorodeoxyglucose (^{18}F -FDG) positron emission tomography/computed tomography (PET/CT) to evaluate early TAVI valve degeneration.

PATIENTS AND METHODS In this prospective study with a prespecified follow-up protocol, 71 TAVI patients underwent baseline transthoracic and transesophageal echocardiography, and PET/CT with ^{18}F -NaF and ^{18}F -FDG. Of these, 31 patients completed 24-month control examinations, while the others were lost to mortality and the COVID-19 pandemic. We measured PET tracer activity and compared ^{18}F -NaF and ^{18}F -FDG PET/CT uptake at baseline and 24-month follow-up.

RESULTS PET/CT and echocardiography data were analyzed for 31 of the 71 enrolled TAVI patients at a median age of 84 years (interquartile range, 80–86). After TAVI, an improvement in the valve function was observed. During follow-up, the valve function remained stable. PET/CT demonstrated an increase in ^{18}F -FDG maximal uptake in the inner (tissue-to-background ratio, $P = 0.009$) and outer ($P = 0.01$) sides of the TAVI valve stent, but no difference in ^{18}F -NaF maximal activity (inner, $P = 0.17$; outer, $P = 0.57$).

CONCLUSIONS Twenty-four months post-TAVI, an increase in ^{18}F -FDG uptake, indicative of inflammation, was observed in the valve, while the uptake of the calcification marker (^{18}F -NaF) remained stable. These observations might suggest early stages of TAVI valve degeneration, although further investigation is required to confirm this interpretation.

INTRODUCTION The prevalence of degenerative aortic stenosis (AS) increases with age, and transcatheter aortic valve implantation (TAVI) has

become a standard treatment for patients at higher surgical risk. However, due to expanding indications and application of TAVI in moderate- or

Correspondence to:

Danuta Sorysz, MD, PhD,
Second Department of Cardiology,
Institute of Cardiology, Jagiellonian
University Medical College,
ul. Jakubowskiego 2, 30-688 Kraków,
Poland, phone: +48 12 400 22 50,
email: danuta.sorysz@uj.edu.pl
Received: July 5, 2023.

Revision accepted: August 23, 2023.

Published online:

November 15, 2023.

Pol Arch Intern Med. 2023;

133 (12): 16607

doi:10.20452/pamw.16607

Copyright by the Author(s), 2023

WHAT'S NEW?

The study investigated the potential of ^{18}F -sodium fluoride (^{18}F -NaF) and ^{18}F -fluorodeoxyglucose (^{18}F -FDG) positron emission tomography/computed tomography (PET/CT) imaging to detect early signs of degeneration in transcatheter aortic valve implantation (TAVI) valves, offering new insights into the initial stages of the valve degeneration. Our findings demonstrate that increased uptake of ^{18}F -FDG, an inflammation marker, is observed 24 months after TAVI, while the uptake of a calcification marker, ^{18}F -NaF, remains stable. This suggests that inflammation may play a pivotal role in the early stages of the TAVI valve degeneration. Our unique approach of obtaining baseline PET data 6 months after TAVI, followed by a control examination at 24 months, highlights the potential of PET/CT imaging as a valuable diagnostic tool for monitoring TAVI valve degeneration and guiding future research into novel therapies.

even low-risk patients, understanding the factors affecting durability of these valves is crucial.¹⁻⁶ While the TAVI valve degeneration has been less extensively studied than that of bioprosthetic aortic valves,⁷ some reports suggest their similar durability.⁸ Conversely, crimping of the TAVI valve may present as a risk factor for its accelerated degeneration. Additionally, eccentric stent opening under unfavorable anatomical conditions, which can result in asymmetric leaflet movement, may contribute to an increased risk of the valve deterioration. This raises questions about the initiation, mechanisms, and risk factors for the valve degeneration, and potential strategies for slowing down this process. Therefore, we aimed to assess the utility of positron emission tomography (PET)/computed tomography (CT) in evaluating the early stages of the TAVI valve degeneration and gaining insights into the underlying inflammatory and calcification mechanisms.

PATIENTS AND METHODS **Study population** A total of 71 consecutive patients with symptomatic severe AS, who qualified for TAVI, were prospectively enrolled in this single-center, observational study from July 2017 to January 2020.^{9,10} Our research protocol included a baseline visit (2 days before TAVI) and follow-up clinical visits at 1, 6, 12, and 24 months, accompanied by transthoracic echocardiography (TTE) examinations (FIGURE 1). PET/CT and transesophageal echocardiography (TEE) were performed at the 6-month visit, and initially planned for the final, 24-month follow-up visit; however, due to the COVID-19 pandemic, some patients experienced delays. Consequently, a large proportion of clinical follow-up with TTE was also abandoned in this high-risk population. FDG-labeled PET/CT examinations were delayed in patients diagnosed with thrombosis until valve morphology was normalized. The final PET/CT results were then compared with the initial PET/CT data.

Echocardiography All patients underwent TTE, encompassing 2-dimensional (2D), 3-dimensional

(3D), and Doppler imaging, at baseline and during follow-up. Acquisition settings were meticulously optimized to ensure maximal image quality. To enhance visualization of the TAVI valve leaflets, 2D and 3D TEE were conducted at the 6-month and final follow-up visits. TTE and TEE examinations were performed using Vivid E9 and Vivid E95 devices (GE Healthcare, Waukesha, Wisconsin, United States). Postprocessing evaluations were carried out on a dedicated workstation (EchoPAC, GE Healthcare), with linear measurements taken with virtual calipers. TTE examinations and measurements adhered to the recommendations for assessing AS and TAVI valves.^{11,12} TEE visual assessments of the aortic valve morphology and leaflet movements were performed. All measurements were independently validated by a core laboratory (KCRI, Kraków, Poland).

Positron emission tomography computed tomography Electrocardiography (ECG)-gated and breathless PET/CT scans of the TAVI valves were performed using ^{18}F -fluorodeoxyglucose (^{18}F -FDG) and ^{18}F -sodium fluoride (^{18}F -NaF) with the GE Discovery 690 VCT scanner (GE Healthcare).^{9,10} ^{18}F -NaF and ^{18}F -FDG were administered intravenously at a dose of 4 MBq per kg of body mass (followed by a 60-minute rest in a quiet environment), with acquisition performed as described above. An attenuation-corrected CT scan (nonenhanced, ECG-gated, low-dose 120 kV with modulated rays [Smart mA] range 80 to 220 mAs) was performed, followed by PET imaging covering a 15 cm single-bed position centered over the valve in 3D mode for 16 minutes. The PET data were reconstructed using the GE reconstruction algorithm (matrix size, 128×128 , Vue Point FX: 24 subsets, 2 iterations with a 12 mm cutoff Cardiac 3D filter for static images; Vue Point FX: 24 subsets, 5 iterations with a 4.3 mm cutoff Cardiac 3D filter for gated images). Corrections were applied for attenuation, dead time, scatter, and random coincidences. Upon PET reconstruction, we obtained 8-bin CT-gated PET images. CardIQ Fusion PET software (GE Healthcare) was used for the image analysis.

All image analyses were performed on fused PET/CT datasets. For both ^{18}F -FDG PET/CT and ^{18}F -NaF PET/CT scans, measurements were performed as described below (FIGURE 2A-2D). ECG-gated PET/CT scans were used to increase reliability of the results, with measurements taken during diastole, when the valve leaflets had the highest chance of being closed. 3D multiplanar reconstruction mode was used to visualize the valve in the coaxial short-axis view, for more precise delineation of the regions of interest (ROI) around the valve. In all cases, the mediastinal blood pool subject (MBPS) in the right atrium (RA), maximal standardized uptake value (SUV), mean SUV, and mean density in Hounsfield units were measured. The initial measurements were performed at the level of the closed leaflets (informed by CT stent visualization and

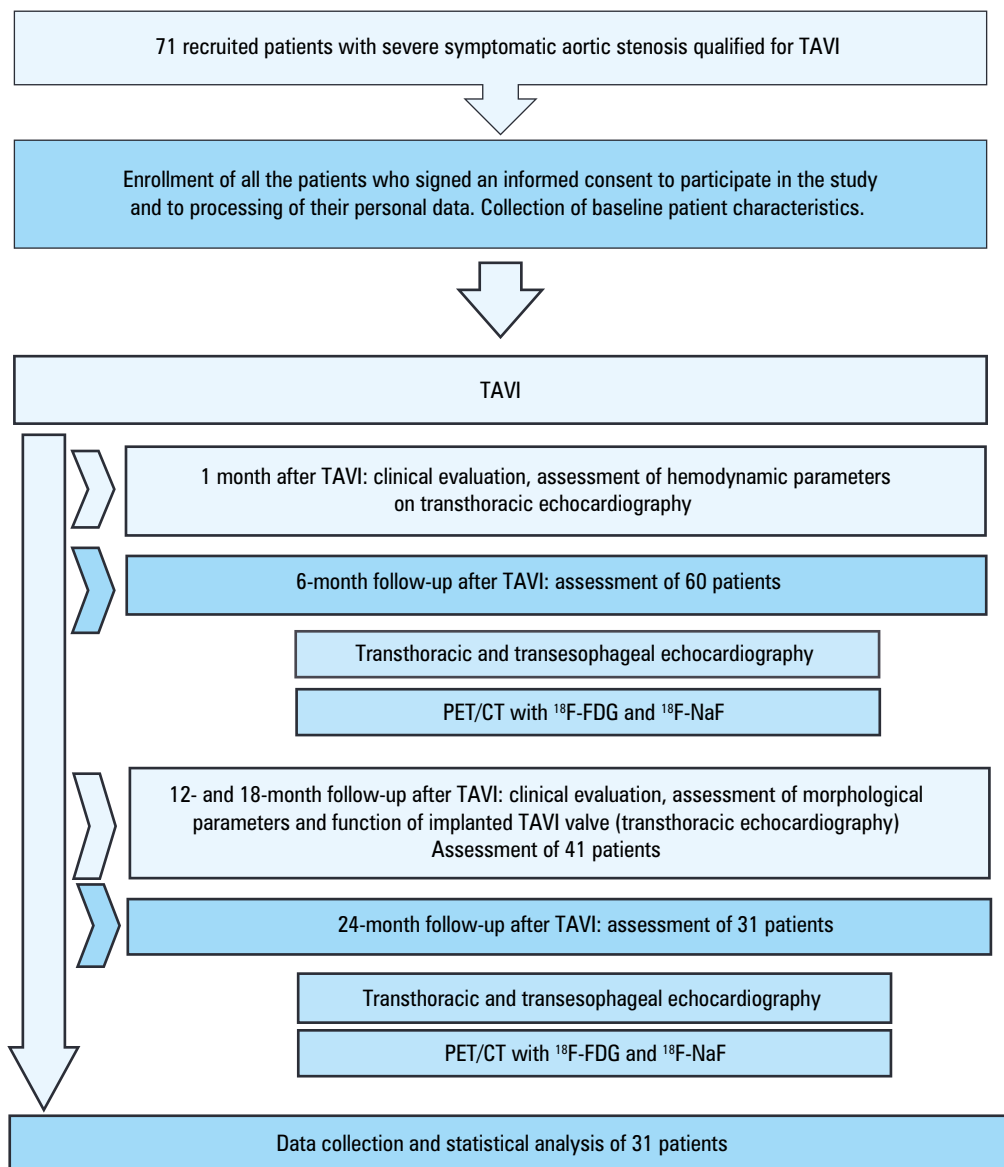


FIGURE 1 Study flow chart

Abbreviations: ^{18}F -FDG, ^{18}F -fluorodeoxyglucose; ^{18}F -NaF; ^{18}F -sodium fluoride; PET/CT, positron emission tomography/computed tomography; TAVI, transcatheter aortic valve implantation

TAVI valve manufacturers). The ROIs (according to the stent shape) inside and outside of the stent were drawn, followed by the ROIs on 2 adjacent slices (up and down) to increase the chance of the entire valve examination. The term “inner area” is used to define the area inside the valve (including its leaflets but excluding the valve stent and the aortic annulus), and the outer area contains the valve leaflets, the aortic annulus, and the native leaflets (FIGURE 2A–2D). Mean and maximal SUVs were calculated for each slice, the inner and outer region, and the mean value was determined for all levels of the valve as well as for the inner and outer ROIs. However, SUV measurements in vascular structures are influenced by intraexamination variations of ^{18}F -FDG and ^{18}F -NaF activity in the blood pool. Therefore, subtraction SUV values of the ROIs, as well as background tracer uptake in MBPS and blood pool in the RA were measured and analyzed according to the suggestions from previously published

papers.¹³ The gathered data included mean and maximum tissue-to-background ratios (TBRs).¹³ These ratios help minimize the influence of individual SUVs (SUV_{max} and SUV_{mean}) on the results.

The study received ethics approval from the Institutional Review Board of the Jagiellonian University Medical College (1072.6120.90.2017), and written informed consent was obtained from all participants. The study protocol followed the ethical standards set out in the 1975 Declaration of Helsinki.

Statistical analysis Categorical variables are presented as numbers and percentages, while continuous variables are expressed as either mean (SD) or median (interquartile range [IQR]), as appropriate. The Shapiro–Wilk test was used to assess normality, and the Levene test was applied to evaluate the equality of variances. For the normally distributed variables, differences between the baseline and follow-up parameters

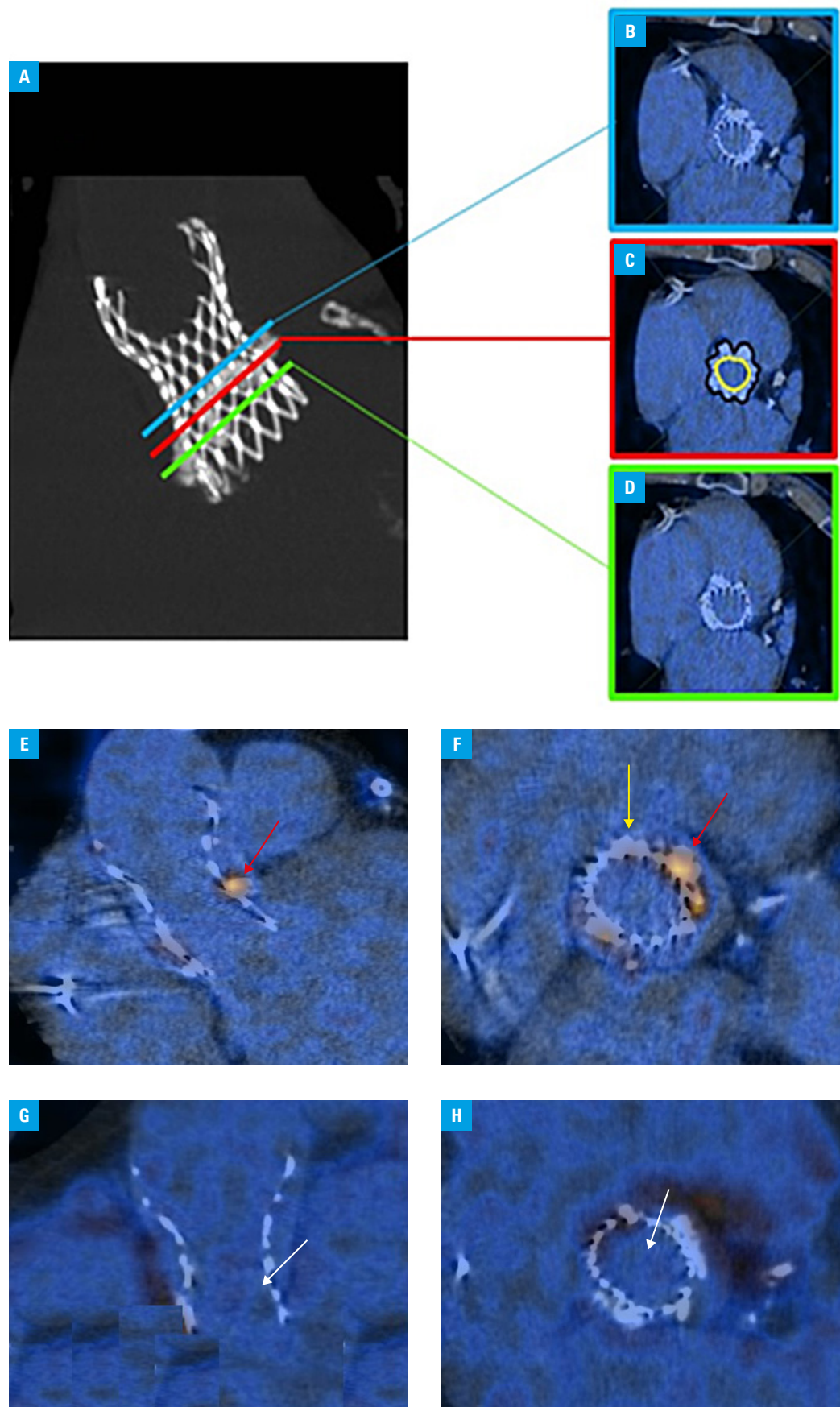


FIGURE 2 **A** – computed tomography (CT) image of a transcatheter aortic valve implantation (TAVI) valve used to assess the level of the valve leaflets; **B** – blue line, upper slice of the analysis; **C** – red line, initial level of the analysis, yellow region of interest (ROI) shows the area inside the valve stent, black ROI shows the area outside with the annulus and native leaflet calcifications. **D** – green line, lower level of the analysis; **E, F** – long and short axis of the TAVI valve visualized with ^{18}F -sodium fluoride positron emission tomography (PET)/CT showing local uptakes out of the valve (red arrow) and calcification without uptake (yellow arrow); **G, H** – long and short axis of the TAVI valve visualized with ^{18}F -fluorodeoxyglucose PET/CT showing no uptake at the level of the leaflets (white arrows)

TABLE 1 Baseline demographic and clinical characteristics

Parameter	All patients (n = 71)	Patients with follow-up (n = 31)
Age, y, median (IQR)	84 (80–87)	84 (80–86)
Male sex, n (%)	29 (40.9)	11 (35.5)
Weight, kg, mean (SD)	71.9 (14.9)	72 (14.2)
Height, cm, mean (SD)	163.5 (9.5)	162.3 (8.5)
Body mass index, kg/m ² , mean (SD)	26.8 (4.6)	27.2 (4.4)
Body surface area, m ² , mean (SD)	1.8 (0.2)	1.7 (0.1)
eGFR, ml/min/1.73 m ² , median (IQR)	64.5 (48–78)	66 (52–82)
eGFR <60 ml/min/1.73 m ² , n (%)	33 (35.5)	10 (32.3)
NYHA class, n (%)	I	2 (2.8)
	II	15 (21.1)
	III	47 (66.2)
	IV	7 (9.9)
Arterial hypertension, n (%)	62 (87.3)	27 (87.1)
Diabetes mellitus, n (%)	28 (39.4)	15 (48.3)
Atrial fibrillation, n (%)	39 (54.9)	17 (54.8)
Previous myocardial infarction, n (%)	25 (35.2)	11 (35.4)
Previous percutaneous coronary intervention, n (%)	30 (42.25)	15 (48.3)
Previous coronary artery bypass grafting, n (%)	12 (16.9)	7 (22.5)
Previous balloon aortic valvuloplasty, n (%)	28 (39.4)	11 (35.4)
Chronic obstructive pulmonary disease, n (%)	10 (14.1)	5 (16.1)
Previous stroke/TIA, n (%)	10 (14.1)	4 (12.9)
Previous pacemaker implantation, n (%)	12 (16.9)	6 (19.3)

Abbreviations: eGFR, estimated glomerular filtration rate; IQR, interquartile range; NYHA, New York Heart Association; TIA, transient ischemic attack

TABLE 2 Baseline and follow-up echocardiographic data

Parameter	Before TAVI (n = 31)	1 month (n = 27)	<i>P</i> value ^a	12 months (n = 25)	<i>P</i> value ^b	24 months (n = 31)	<i>P</i> value ^c
PG, mm Hg, mean (SE)	85.3 (3.1)	17 (3.3)	<0.001	16.9 (3.4)	0.99	14.8 (3.1)	0.97
MPG, mm Hg, mean (SE)	51.1 (2)	9.4 (2.1)	<0.001	9.1 (2.2)	0.99	8 (2)	0.98
AVA, cm ² , mean (SE)	0.6 (0.1)	1.6 (0.1)	<0.001	1.5 (0.1)	0.82	1.5 (0.1)	0.99
AVAi, cm ² /m ² , mean (SE)	–	0.91 (0.04)	–	0.88 (0.04)	0.43	0.88 (0.04)	0.98
LVEF, %, mean (SE)	50.5 (2.6)	55.7 (2.6)	0.02	56 (2.7)	0.99	54.1 (2.6)	0.71
sPAP, mm Hg, mean (SE)	55.6 (3)	51 (3.3)	0.62	51 (3.8)	0.99	46.8 (3.4)	0.77
AR, n (%)							
None	1 (3.2)	3 (11.1)	0.99	3 (12)	0.99	6 (19.4)	0.99
Trace	8 (25.8)	4 (14.8)		5 (50)		7 (22.6)	
Mild	15 (48.4)	14 (51.9)		12 (48)		14 (45.2)	
Moderate	4 (12.9)	6 (22.2)		5 (20)		4 (12.9)	
Severe	3 (9.7)	0		0		0	

a Before TAVI vs 1 month

b 1 vs 12 months

c 1 vs 24 months

Abbreviations: AR, aortic regurgitation; AVA, aortic valve area; AVAi, aortic valve area index; LVEF, left ventricular ejection fraction; MPG, mean transvalvular gradient; PG, maximal transvalvular pressure gradient; sPAP, systolic pulmonary artery pressure; others, see [FIGURE 1](#)

were compared using the mixed effect models. The Pearson χ^2 test or the Fisher exact test was used to compare the categorical variables, with the latter applied if 20% of cells had an expected count of less than 5 (the Monte Carlo simulation was utilized for the Fisher test in the cases with dimensions exceeding 2×2 tables). Intra-class correlation coefficients were computed to evaluate the intraobserver variability in the analysis of ¹⁸F-FDG and ¹⁸F-NaF activity. Two-sided *P* values below 0.05 were considered significant. All analyses were performed using R 4.2.3 software (R Foundation for Statistical Computing, Vienna, Austria), with “lme4” package, version 1.1–30 and “emmeans” package, version 1.8.2.

RESULTS General characteristics We recruited 71 patients with TAVI valves, and the final ¹⁸F-NaF and ¹⁸F-FDG PET/CT scans were performed for 31 of them. All the patients were followed up with clinical visits and TTE examinations ([FIGURE 1](#)). Due to the COVID-19 pandemic-related constraints, the median (IQR) time interval from the baseline PET scan, conducted 6 months post-TAVI, to the follow-up PET/CT scan was 18.1 (15.5–21.8) months for ¹⁸F-NaF, and 18.5 (15–26.7) months for ¹⁸F-FDG. Baseline clinical characteristics of the patients are presented in [TABLE 1](#), and ECG data can be found in [TABLE 2](#). In our study group, we identified 5 types of aortic valves used during TAVI: 71% of the patients had the Evolut R valve (Medtronic, Minneapolis, Minnesota, United States), 16.1% had the Accurate Neo valve (Boston Scientific SciMed

Inc., Maple Grove, Minnesota, United States), 6.4% had the SAPIEN 3 valve (Edwards Lifesciences, Irvine, California, United States), 6.4% had the Evolut PRO valve (Medtronic), and 12.8% had the Portico valve (St. Jude Medical, Minneapolis, Minnesota, United States). We observed a 9.6% mortality rate at 1 month, 13.7% at 6 months, and 45% at 68 months. Eight patients refused to attend the follow-up visits due to the fear of contracting COVID-19. Asymptomatic valve thrombosis was diagnosed at 6 months in 8.4% of patients (6 cases), and the baseline PET/CT examinations were postponed until the thrombotic lesions resolved. Control PET/CT were ultimately performed in only 3 out of 6 cases. Seven patients declined the 6-month on-site follow-up visit due to the COVID-19 pandemic.

Echocardiography We observed a decrease in both maximal and mean transvalvular gradients, as well as an increase in the effective orifice area and ejection fraction after TAVI. No changes in the valvular parameters were observed at 6, 12, and 24-month follow-up (TABLE 2). At 6 months, TEE revealed thickening and a slight reduction of the leaflet motion in 6 patients; however, anticoagulant therapy resolved these abnormalities. Thrombosis of the TAVI valve was noticed in 1 patient with the Accurate Neo, 2 patients with the Edwards SAPIEN 3 valve, and 1 patient with the Evolut R valve at 6 months. PET/CT examination was postponed until the valve parameters normalized. Similarly, ECG parameters assessed after the resolution of thrombotic features were included in the analysis.

¹⁸F-sodium fluoride and ¹⁸F-fluorodeoxyglucose positron emission tomography/computed tomography The reliability analysis demonstrated an excellent agreement between the observers for both mean and maximal ¹⁸F-FDG and mean and maximal ¹⁸F-NaF activity, with the intraclass correlation coefficients ranging from 0.986 to 0.993. Analysis of microinflammation assessed by ¹⁸F-FDG uptake showed similar or increasing values on follow-up PET/CT (TABLES 3 and 4). Differences between absolute SUVs were observed only for SUV_{mean}, while SUV_{max} remained similar on both PET/CTs. The microinflammatory process was comparable in the inner areas of the leaflets of the bottom valve segments and middle valves segments (TABLE 3). An increase in absolute SUV_{mean} of ¹⁸F-FDG uptake was observed for the outer area in the middle segments (TABLE 3). The averaged absolute SUV_{max} and SUV_{mean} for the TAVI valves counted at baseline and follow-up PET/CT did not show differences; however, the analysis of averaged corrected SUV_{max} values: SUV_{max} TBR-RA showed differences between the baseline and follow-up PET/CT. This relationship was not observed for the averaged corrected SUV_{mean} (TABLE 4).

The analysis of microcalcification evaluated by ¹⁸F-NaF PET/CT showed no differences between

the absolute SUV_{max} or SUV_{mean} of the inner and outer areas, independently of the mapping level (TABLE 3). The averaged absolute SUV_{max} and SUV_{mean} of the ¹⁸F-NaF uptake for the TAVI valves counted at baseline and follow-up PET/CT did not show differences. In addition, there were no differences between baseline and follow-up PET/CTs, when comparing the averaged values of corrected ¹⁸F-NaF uptake in the TAVI valves (TABLE 4).

DISCUSSION Our study facilitates understanding of the degenerative process in the TAVI valves by providing insights into its early stages. We demonstrated that, within an average of 24 months following TAVI, increased activity on PET/CT scans is detectable only for ¹⁸F-FDG, that is, the inflammation marker, with no change in the activity of ¹⁸F-NaF, the microcalcification marker. ECG performed during follow-up revealed no changes in the valve functional parameters, indicating no hemodynamically significant degenerative changes. The ECG parameters evaluate the valve functional change, when the leaflet mobility is impaired, which is not the case at the early stage of degeneration. However, these parameters were clearly altered in the patients diagnosed with asymptomatic valvular thrombosis.

Valve degeneration is a long-term process, and its initial stages involve local inflammatory changes, including infiltration of inflammatory cells. Microdamage to the endothelium, which may be associated with crimping in the TAVI valves, is one of the initiating factors. At later stages of degeneration, abnormalities progress into osteogenic differentiation and calcification.¹⁴⁻¹⁶ Dweck et al¹⁷ demonstrated higher ¹⁸F-FDG activity at subsequent stages of AS, detectable at the stage of sclerosis, while increased uptake of ¹⁸F-NaF was associated with calcification at advanced stages of the valve degeneration. In contrast, Almerri et al¹⁴ reported increased perivalvular ¹⁸F-FDG uptake shortly after TAVI (7 days) as an inflammatory response to the valve implantation injury. To account for this potential phenomenon, we performed baseline PET/CT scan 6 months after TAVI, ensuring that the tissue healing did not influence the results. Consequently, the observed increase in ¹⁸F-FDG activity in our study during the control PET/CT scan at 30 months may indicate local inflammation. However, it still remains to be determined whether these changes result in clinically significant valve degeneration. Contrary to the findings of Dweck et al,¹⁷ we did not observe either increased ¹⁸F-NaF uptake on the control PET/CT scans or its elevated values. This discrepancy may be attributed to the valve age. All patients in our study had control examinations at about 24 months from the implantation (“young” valves), while 81% of the patients in Dweck’s group had valves older than 24 months, including 34% at 5 years post-implantation. This factor increased the likelihood

TABLE 3 Differences between standardized uptake values on positron emission tomography/computed tomography between the baseline and follow-up obtained at different mapping levels

Parameter	¹⁸ F-FDG		P value	¹⁸ F-NaF		P value	
	Baseline (n = 31)	Follow-up (n = 31)		Baseline (n = 31)	Follow-up (n = 31)		
SUV inner							
Bottom	Mean	2.2 (2–2.5)	2.4 (2.2–2.6)	0.05	1.9 (1.6–2.1)	1.8 (1.6–2.3)	0.88
	Max	3.9 (3.4–4.7)	3.9 (3.4–4.9)	0.49	3.7 (2.8–4.3)	3.8 (2.9–4.7)	0.86
Middle	Mean	2.2 (2–2.4)	2.3 (2.2–2.6)	0.05	2.1 (1.7–2.3)	2 (1.5–2.5)	0.56
	Max	3.6 (3.2–4.3)	4 (3.2–4.4)	0.13	3.9 (3.3–5)	3.7 (3.1–4.8)	0.34
Top	Mean	2.4 (2–2.7)	2.4 (2.1–2.6)	0.78	2 (1.8–2.2)	2 (1.6–2.5)	0.56
	Max	3.5 (3.2–4.4)	3.9 (3.3–4.4)	0.38	4.1 (3.3–4.5)	3.8 (3.1–5.4)	0.64
SUV outer							
Bottom	Mean	2.2 (2.1–2.7)	2.4 (2.1–2.6)	0.51	2 (1.6–2.3)	2 (1.6–2.4)	0.91
	Max	4.5 (3.9–5.5)	4.4 (3.6–5.3)	0.38	4.2 (3.8–5.9)	4.4 (3–5.4)	0.26
Middle	Mean	2.2 (2–2.5)	2.4 (2.2–2.6)	0.04	2.2 (1.9–2.6)	2 (1.8–2.5)	0.42
	Max	4.3 (3.8–5.4)	4.2 (3.7–4.8)	0.26	5.1 (4.5–6.3)	4.9 (3.6–6.2)	0.59
Top	Mean	2.3 (2.1–2.6)	2.4 (2.1–2.5)	0.53	2.1 (1.9–2.6)	2.1 (1.8–2.7)	0.47
	Max	3.4 (2.9–4.2)	4.2 (3.7–4.9)	0.02	4.6 (4.3–5.7)	4.6 (3.7–6.1)	0.34
RA, HU		(38.4–53.9)	40.7 (36.1–49.5)	0.16	48.8 (41–51.6)	46 (38–51.6)	0.26

Data are presented as median (interquartile range).

Abbreviations: HU, Hounsfield units; RA, right atrium; SUV, standardized uptake value; others, see [FIGURE 1](#)

TABLE 4 Differences between standardized uptake values on positron emission tomography/computed tomography between baseline and follow-up

Parameter	¹⁸ F-FDG		P value	¹⁸ F-NaF		P value
	Baseline (n = 31)	Follow-up (n = 31)		Baseline (n = 31)	Follow-up (n = 31)	
SUV _{max}	4.1 (3.5–4.7)	4.2 (3.6–4.7)	0.71	4.6 (3.9–5.2)	4.2 (3.2–5.4)	0.34
SUV _{mean}	2.3 (2.1–2.5)	2.4 (2.1–2.6)	0.33	2 (1.8–2.3)	2.01 (1.7–2.6)	0.85
SUV _{max} TBR-RA	1.2 (1–1.7)	1.7 (1.5–2.1)	<0.001	1.6 (1.3–1.9)	1.7 (1.3–2.2)	0.29
SUV _{mean} TBR-RA	1.1 (1–1.3)	1.2 (1–1.3)	0.25	1.2 (1–1.3)	1.3 (0.9–1.5)	0.42
SUV _{max} TBR-RA outer	1.3 (1.1–1.7)	1.7 (1.5–2.1)	0.01	1.7 (1.5–2.3)	1.9 (1.5–2.4)	0.57
SUV _{mean} TBR-RA outer	1.1 (1–1.3)	1.2 (1–1.3)	0.43	1.2 (1–1.4)	1.3 (1–1.5)	0.9
SUV _{max} TBR-RA inner	1.2 (1–1.7)	1.7 (1.5–2.1)	0.009	1.4 (1.1–1.7)	1.5 (1.1–2)	0.17
SUV _{mean} TBR-RA inner	1.1 (0.9–1.3)	1.2 (1.1–1.3)	0.11	1.1 (0.9–1.2)	1.2 (0.9–1.4)	0.42

Data are presented as median (interquartile range)

Abbreviations: TBR-RA, tissue-to-background ratio–right atrium; others, see [FIGURE 1](#) and [TABLE 3](#)

of detecting dynamic changes in ¹⁸F-NaF uptake. Our results suggest that calcification may begin more than 24 months after implantation. On the other hand, ¹⁸F-NaF uptake was higher in the AS patients than in the controls and increased progressively with more advanced stages of AS.¹⁷ Increased ¹⁸F-FDG activity was also detected, but with lower values than for ¹⁸F-NaF, and only a mild correlation with the disease severity. At the more advanced stages of the valve dysfunction, calcification, rather than inflammation, played a more important role in the disease progression.¹⁷

Valve calcification is also a stepwise process, starting with microcalcifications, then gradually enhancing until the presence of metabolically inactive calcifications.¹⁸ Analyzing CT images, we observed the presence of large calcifications

in the aortic annulus and native leaflets; however, the use of the ¹⁸F-NaF marker on PET/CT was not always associated with its accumulation in the calcifications, which proves a lack of their metabolic activity ([FIGURE 2E](#) and [2F](#)). Similarly, the analyses of atherosclerotic lesions in the coronary arteries showed that active ¹⁸F-NaF uptake was associated with a 20-fold higher risk of calcification progression (calcium score) than in the case of the atherosclerotic plaques not showing active ¹⁸F-NaF uptake.^{18,19} In patients after carotid endarterectomy, increased ¹⁸F-NaF activity was associated with the histological presence of hydroxyapatite.²⁰

Exploring the limitations and challenges of PET/CT imaging in the context of TAVI valve degeneration is crucial for understanding the feasibility of implementing this technique in clinical practice. Several challenges of PET/CT imaging

need to be addressed, including high cost, limited access, and radiation exposure. Alternative imaging modalities, such as PET/magnetic resonance imaging, could potentially reduce the radiation exposure and still provide necessary diagnostic information. Another challenge is a relatively long time necessary for PET/CT imaging, which can be inconvenient for patients and health care providers. Lastly, standardization of imaging procedures is critical to address variability in PET/CT imaging protocols that can lead to inconsistent image quality and reduced diagnostic accuracy. Establishing standardized procedures, including administration of radiotracers, patient preparation, and image acquisition and analysis, is necessary to ensure high-quality, repeatable results across different imaging centers. These limitations mean that this method requires further evaluation before possible introduction to a wider audience.

A unique aspect of our study is the acquisition of baseline PET data 6 months from TAVI, followed by control examinations approximately 18 months later, utilizing both ^{18}F -NAF and ^{18}F -FDG. Confirming increased ^{18}F -FDG uptake, which may correspond to the initial degenerative changes in the TAVI valve, raises the possibility of employing this diagnostic imaging method to evaluate the efficacy of novel molecules in inhibiting AS progression. Establishing a correlation between PET/CT findings, particularly changes in ^{18}F -FDG and ^{18}F -NaF activity, with clinical outcomes such as valve durability, morbidity, and mortality would further validate the usefulness of PET/CT imaging in assessing TAVI valve degeneration.

Our study has several limitations. The primary constraint is the small size of the study group, which increases the risk of selection bias. Unfortunately, the COVID-19 pandemic made it impossible to collect data from the initially planned 80 patients. The relatively short observation period may have been insufficient to obtain definitive confirmation of TAVI valve degeneration progress. Additionally, the PET method employed has certain limitations regarding temporal and spatial resolution. Despite its innovative aspect, it remains technically challenging for studies investigating bioprosthetic valve degeneration.

Conclusions In conclusion, our study identified an increased uptake of ^{18}F -FDG, potentially indicative of local inflammation that may precede the onset of calcification as detectable by ^{18}F -NaF uptake. However, the significance of this phenomenon and its connection with valve degeneration remains to be definitively established. These findings underscore the potential of PET/CT imaging as a valuable tool for monitoring local inflammation, which could represent an early stage of the degenerative process in TAVI valves, and for guiding future research toward development of novel therapies to impede the progression of AS. However, given the limitations of the imaging

method described and the size of the study group, additional studies involving larger patient populations and extended follow-up periods are necessary to confirm our findings and ascertain the clinical implications of PET/CT imaging in assessing the TAVI valve degeneration.

ARTICLE INFORMATION

ACKNOWLEDGMENTS None.

FUNDING The study was supported by a grant from the Polish National Science Center (2016/23/B/NZ5/01460; to DD).

CONTRIBUTION STATEMENT DS is the author of the research concept and design. AD and DS analyzed the data. KPM performed the statistical analysis. MO, ASS, AG, and DS performed and interpreted the analysis of the PET/CT images. MP, NM, and KPM collected the data. All authors participated in drafting the article or revising it critically for important intellectual content, and gave final approval of the version to be submitted.

CONFLICT OF INTEREST None declared.

OPEN ACCESS This is an Open Access article distributed under the terms of the Creative Commons Attribution-NonCommercial-ShareAlike 4.0 International License ([CC BY-NC-SA 4.0](https://creativecommons.org/licenses/by-nc-sa/4.0/)), allowing third parties to copy and redistribute the material in any medium or format and to remix, transform, and build upon the material, provided the original work is properly cited, distributed under the same license, and used for noncommercial purposes only.

HOW TO CITE Sorysz D, Dziewierz A, Opalińska M, et al. ^{18}F -fluorodeoxyglucose and ^{18}F -sodium fluoride positron emission tomography imaging in assessing early stages of aortic valve degeneration after transcatheter aortic valve implantation. *Pol Arch Intern Med.* 2023; 133: 16607. doi:10.20452/pamw.16607

REFERENCES

- 1 Eggebrecht H, Mehta RH. Transcatheter aortic valve implantation (TAVI) in Germany: more than 100,000 procedures and now the standard of care for the elderly. *EuroIntervention.* 2019; 14: e1549-e1552. [↗](#)
- 2 Dąbrowski M, Parma R, Huczek Z, et al. The Polish Interventional Cardiology TAVI Survey (PICTS): 10 years of transcatheter aortic valve implantation in Poland. The landscape after the first stage of the Valve for Life Initiative. *Pol Arch Intern Med.* 2021; 131: 413-420. [↗](#)
- 3 Hájek P, Poláková E, Adlová R, et al. Mid-term outcomes of patients with Lotus and Evolut transcatheter valves. *Adv Cardiol Interv.* 2022; 18: 146-153. [↗](#)
- 4 Bruno F, D'Ascenzo F. Transcatheter aortic valve implantation in Poland: the journey of a thousand miles begins with a single step. *Pol Arch Intern Med.* 2021; 131: 407-408. [↗](#)
- 5 Marzec K, Jaworska-Wilczyńska M, Kowalik I, et al. Comparison of long-term outcomes and risk factors of aortic stenosis treatment in patients undergoing transcatheter aortic valve implantation and surgical aortic valve replacement. *Kardiol Pol.* 2022; 80: 792-798. [↗](#)
- 6 Huczek Z, Rymuza B, Mazurek M, et al. Temporal trends of transcatheter aortic valve implantation in a high-volume academic center over 10 years. *Kardiol Pol.* 2021; 79: 820-826. [↗](#)
- 7 Cartlidge TRG, Doris MK, Sellers SL, et al. Detection and prediction of bioprosthetic aortic valve degeneration. *J Am Coll Cardiol.* 2019; 73: 1107-1119. [↗](#)
- 8 Kwiecinski J, Tzolos E, Cartlidge TRG, et al. Native aortic valve disease progression and bioprosthetic valve degeneration in patients with transcatheter aortic valve implantation. *Circulation.* 2021; 144: 1396-1408. [↗](#)
- 9 Sorysz D, Dziewierz A, Staszczak A, et al. Unusual rapid progression of TAVI valve degeneration confirmed on PET-CT scan after the valve-in-valve procedure followed by early valve thrombosis. *Pol Arch Intern Med.* 2023; 133: 16454. [↗](#)
- 10 Sorysz D, Januszek R, Sowa-Staszczak A, et al. The usefulness of [^{18}F] F-fluorodeoxyglucose and [^{18}F] F-sodium fluoride positron emission tomography imaging in the assessment of early-stage aortic valve degeneration after transcatheter aortic valve implantation (TAVI)-protocol description and preliminary results. *J Clin Med.* 2021; 10: 431. [↗](#)
- 11 Baumgartner H, Hung J, Bermejo J, et al. Recommendations on the echocardiographic assessment of aortic valve stenosis: a focused update from the European Association of Cardiovascular Imaging and the American Society of Echocardiography. *Eur Heart J Cardiovasc Imaging.* 2017; 18: 254-275. [↗](#)
- 12 Hahn RT, Leipsic J, Douglas PS, et al. Comprehensive echocardiographic assessment of normal transcatheter valve function. *JACC Cardiovasc Imaging.* 2019; 12: 25-34. [↗](#)
- 13 Pawade TA, Cartlidge TR, Jenkins WS, et al. Optimization and reproducibility of aortic valve 18F-fluoride positron emission tomography in patients with aortic stenosis. *Circ Cardiovasc Imaging.* 2016; 9: e005131. [↗](#)
- 14 Almerri K, Garashi M, Panchadar S, et al. Acute uptake of 18F-fluorodeoxyglucose following transcatheter aortic valve replacement: first

documentation of inflammatory response to injury. *AsiaIntervention*. 2022; 8: 150-152. [↗](#)

15 New SE, Aikawa E. Molecular imaging insights into early inflammatory stages of arterial and aortic valve calcification. *Circ Res*. 2011; 108: 1381-1391. [↗](#)

16 Yutzey KE, Demer LL, Body SC, et al. Calcific aortic valve disease: a consensus summary from the Alliance of Investigators on Calcific Aortic Valve Disease. *Arterioscler Thromb Vasc Biol*. 2014; 34: 2387-2393. [↗](#)

17 Dweck MR, Jones C, Joshi NV, et al. Assessment of valvular calcification and inflammation by positron emission tomography in patients with aortic stenosis. *Circulation*. 2012; 125: 76-86. [↗](#)

18 De Azevedo D, Geers J, Gheysens O, et al. ¹⁸F-sodium fluoride PET/CT in assessing valvular heart and atherosclerotic diseases. *Semin Nucl Med*. 2023; 53: 241-257. [↗](#)

19 Doris MK, Meah MN, Moss AJ, et al. Coronary 18F-fluoride uptake and progression of coronary artery calcification. *Circ Cardiovasc Imaging*. 2020; 13: e011438. [↗](#)

20 Fiz F, Piccardo A, Morbelli S, et al. Longitudinal analysis of atherosclerotic plaques evolution: an 18F-NaF PET/CT study. *J Nucl Cardiol* 2022; 29: 1713-1723. [↗](#)